Title
Periodic Magnetic Structure Design Calculations for the ALS U8.0 Undulator (Advanced Light Source)

Authors
Savoy, R.
Hassenzahl, W.V.

Publication Date
1992-03-01

LBL-32025
UC-406
Preprint

Lawrence Berkeley Laboratory

UNIVERSITY OF CALIFORNIA

Accelerator & Fusion Research Division

Submitted to Nuclear Instruments and Methods in Physics Research A

Periodic Magnetic Structure Design Calculations for the ALS U8.0 Undulator

R. Savoy and W.V. Hassenzahl

March 1992

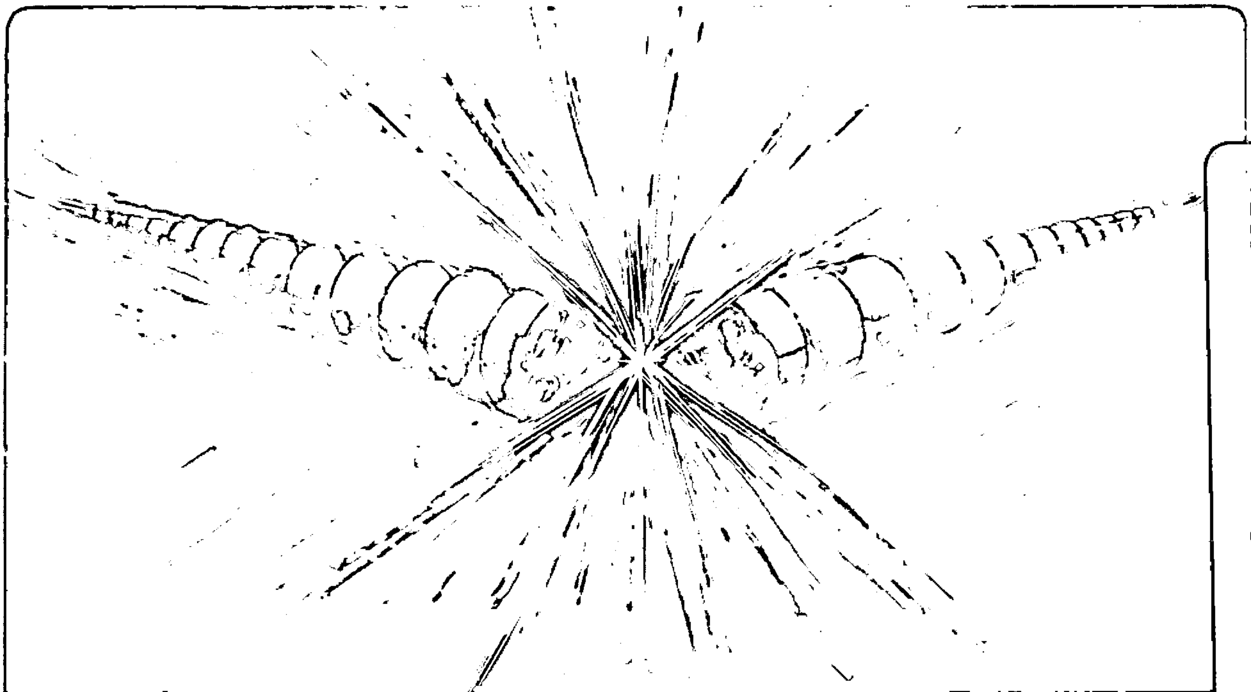

Prepared for the U.S. Department of Energy under Contract Number DE-AC03-76SF00098

DISCLAIMER

LBL-32025

Periodic Magnetic Structure Design Calculations for the ALS U8.0 Undulator*

R. Savoy, W. V. Hassenzahl

Advanced Light Source
Accelerator and Fusion Research Division
Lawrence Berkeley Laboratory
University of California
Berkeley, CA 94720

March 1992

Paper to be submitted to "Nuclear Instruments & Methods in Physics Research"

***This work was supported by the Director, Office of Energy Research, Office of Basic Energy Sciences, Materials Sciences Division of the U.S. Department of Energy, under Contract No. DE-AC03-76SF00098**

Periodic Magnetic Structure Design Calculations for the ALS U8.0 Undulator

R. Savoy, W. V. Hassenzahl

Abstract: The Advanced Light Source at the Lawrence Berkeley Laboratory is scheduled to be commissioned in April 1993. Three insertion devices will be ready for operation at that time, two 5.0 cm period undulators and one 8.0 cm period undulator. This paper describes the parameters of the periodic magnetic structure for the 8.0 cm device, U8.0. We determined these parameters based on a theory of hybrid insertion device design (developed by K. Halbach), which relates the magnetic field to the material characteristics and the geometry of the periodic structure.

Introduction

The U8.0 Undulator is a 55 period, 8 cm period, 4.5 m long hybrid insertion device [1]. It consists of a periodic array of vanadium permendur "steel" poles and Nd-Fe-B permanent magnets to energize the poles. This insertion device (ID) is designed to provide electromagnetic radiation between 6 and 1000 eV on the 1.5-GeV storage ring of the Advanced Light Source (ALS) [2] now under construction at the Lawrence Berkeley Laboratory (LBL). A magnetic field B_{eff} of 1.25 T is required to achieve the low-energy end of this spectral range. This field occurs at the minimum design gap of 14 mm where the peak field peak is 1.38 T. Thus, user requirements and the peak field allowed by machine operation will determine the minimum operating gap. Accelerator performance may be affected by undulators having fields greater than the storage ring bending magnets (1.04 T) corresponding to a photon energy of about 9 eV for U8.0. The present user requirements for photon energy begin at 10 eV, and the lower limit for the initial U8.0 beamline is about 17 eV.

In designing the periodic magnetic structure for U8.0, we followed the procedure developed for the design of the ALS U5.0 Undulator [3], which is based on a theory for the design of hybrid insertion devices [4]. The primary goal of the periodic magnetic structure design effort is to determine the dimensions of the pole and the permanent magnet material (CSEM or Charge Sheet Equivalent Material) that are necessary to achieve the specified B_{eff} with the minimum volume of permanent magnet material.

Though the magnetic structure for an insertion device is three dimensional, most of the tools readily available for field calculations, such as POISSON and PANDIRA [5], are two dimensional. Therefore, the design is split into two phases. The first phase is a set of two-dimensional calculations that: 1. relate the spatial field distribution to the pole thickness, the operating point of the magnetic material, and the saturation state of the pole; 2. determine the relation between the peak magnetic field in the midplane and the flux into the pole due to the CSEM; and 3. determine the impact of the proximity of a steel backing beam on error fields due to material and construction imperfections. In the second phase, the results of these 2D calculations are used to perform the detailed three-dimensional design. In this phase, the theory [4] is used to determine: 1. the pole thickness and height; 2. the overhang of the CSEM at the top and side of the pole; and 3. the engineering tolerances for fabrication and assembly of the magnetic structure and for the magnetic homogeneity of the CSEM blocks.

There are two approaches to the magnetic structure design problem. One is to start with the required B_{eff} and calculate these parameters, the second is to select reasonable values for pole height and overhang and then calculate the resulting fields, iterating until a suitable combination is found. The second approach is chosen here and is implemented in a spread sheet application program [6]. The 2-D and 3-D calculations are summarized in the following sections.

Two-Dimensional Calculation

The 2-D calculation is composed of several distinct parts. Because of the symmetry of the periodic magnetic structure in a planar undulator, one can start by solving for the magnetic field in one quarter period, in particular, the portion that is closest to the electron beam, as shown in Fig. 1. This figure shows the pole of ferromagnetic material, the CSEM, and a current element that is necessary to establish the desired operating point in the CSEM and the resulting field distribution. The coordinate system has the electron beam traveling in the positive z direction, the vertical magnetic field is B_y, and the lateral pole width is along the x direction, which is also the direction of oscillation of the electrons.

The energy of the undulator radiation is a function of the spatial distribution of the magnetic field at the electron beam. The on-axis wavelength of the fundamental harmonic, λ, is given by:

$$\lambda = \frac{\lambda_u}{2\gamma^2}\left(1 + \frac{K^2}{2}\right) ,$$

where γ is the ratio of the electron energy to the electron rest mass (~3000 for the ALS at 1.5 GeV), the undulator period λ_u is in cm, and K is the ID deflection parameter.

$$K = 0.934\ B_{eff}\,\lambda_u = 0.934 \left(\sum_{i=0}^{\infty} \frac{B_{2i+1}^2}{(2i+1)^2}\right)^{1/2} \lambda_u ,$$

where the effective field B_{eff} is in tesla, and we have used the fact that the field distribution in the midplane can be separated into the allowed Fourier components B_{2i+1}, which are the odd harmonics.

The amplitudes of the spatial harmonics B_{2i+1} were determined for various pole widths and for 1 mm and 2 mm chamfer sizes. Chamfers are used to reduce saturation in the corner of the pole (which makes the device less sensitive to material variation), to break the sharp edge for handling, and to reduce the higher harmonics.

The normalized effective field, B_{eff}/B_{peak}, is plotted in Fig. 2 as a function of both pole thickness and normalized pole thickness (i.e., pole thickness divided by the half period), and is listed in Table I. Both B_{eff} and B_{peak} can be extracted from the POISSON output. It is important to calculate this ratio because the 3-D theory gives B_{peak}, whereas the performance of the device depends on B_{eff}. The relative amplitude of the third harmonic, B_3/B_1, is shown in Fig. 3. The normalized fifth and seventh harmonics, shown in Fig. 4, are seen to be less than 1%.

The final results from the 2-D POISSON calculations are the excess flux coefficient (EFC) and the quantity D_4 [4]. The excess flux coefficient is a measure of the amount of flux entering the pole face compared with the flux between two poles and is shown in Fig. 5 as a function of gap. The quantity D_4 is the scalar potential of the pole divided by the peak field. Values of D_4 for different gaps are plotted in Fig. 6. The large variation in D_4 reflects the change in central field as a function of gap. The scalar potential of the pole is determined by the pole height and the CSEM characteristics, and is nearly independent of gap.

Three-Dimensional Calculation

The 3-D design equations developed by Halbach [4] were incorporated into a program QUICKFIELD [6] implemented on Microsoft Excel. The layout of the spreadsheet and some results are shown in Tables IIa-c. QUICKFIELD calculates the peak field based on a set of input parameters. These parameters include the period length and the magnetic properties of the CSEM (B_r and H_c), and the case dependent variables including pole height, the top and side CSEM overhangs, the EFC, and D_4.

Four different pole configurations are evaluated in Tables II a-c. The data in the first two tables are for the minimum operating gap of 14 mm and those in the third are for the commissioning gap of 22 mm. Table IIa contains data for a pole with the measured permeability of vanadium permendur [7], and Tables IIb and IIc contain data for a pole of infinite permeability. In each of the tables, the first column contains the parameters and results for the U8.0 design that we have selected. The second column, lists the parameters for a U8.0 design scaled up linearly from the U5.0 design [3], that is, all critical dimensions are multiplied by a factor of 1.6. Column three contains parameters for a case with a slightly taller pole than the nominal U8.0 design shown in column 1, but with considerable larger top and side overhangs. Column four is for a case with overhang similar to that in column three but with a taller pole. The incentive for this case was to evaluate the performance of a 3 x 3 CSEM block array, with each block 4-cm square, as opposed to the 2 x 3 array of 3.5-cm square blocks for the U5.0 design and the selected U8.0 design. We believe it is important to use several blocks per half-period to allow the selective placement of blocks, which reduces the error fields.

A major conclusion from these calculations is that a pole configuration that has the same transverse pole dimensions as U5.0 (6 cm high and 8 cm wide) will generate an effective field greater than 1.25 T at a 14 mm gap. The practical implication of this observation is that a considerable portion of the design effort and the assembly hardware for the U5.0 undulator can be used for the U8.0 undulator with little or no modification.

The effects of overhang on the central field, the total CSEM volume in the structure and the operating point are given in Table III for the nominal U8.0 pole at the 14 mm gap. The operating point in the uniform field region between the poles is plotted in Fig. 7 as a function of CSEM overhang at the top of the pole.

Finally,we determined the maximum midplane field as a function of pole height, which is given in Fig. 8 for a pole with infinite permeability. It shows the theoretically well understood fact that after a steep initial rise the peak field levels off. The U8.0 pole height chosen, 6 cm, provides a peak field of ~ 1.4 T. To increase the field to 1.6 T would require an increase in pole height to 13 cm, doubling the quantity of CSEM and vanadium permendur. The height increase required for a finite permeability case would be even greater.

A full height model of a U8.0 quarter period using measured vanadium permendur permeability was run on PANDIRA to obtain an estimate of the central field, resulting in the plot shown in Fig. 9. The peak midplane field for the smallest ALS operational magnetic gap (14 mm) and for the ALS commissioning gap (22 mm) are 1.38 and 0.9 T, respectively. The magnetic field in the pole exceeds 2.1 T everywhere in the lowest 1 cm, and the maximum field exceeds 2.4 T near the chamfer.

Comparison with Experiment

A model pole was built and tested to study the U8.0 magnetic characteristics [8]. This pole used a structure originally constructed for the U5.0 [9], in which half of one half-period of the device is contained in an iron structure that provides mirror planes to simulate the symmetry of the periodic structure. The peak field measured in this device at a gap that corresponds to 14 mm in U8.0 was 1.394 T. This value is higher than would be expected in the real U8.0 because the Hall probe was slightly above the midplane, and because the blocks of CSEM were slightly stronger, 11400 G, than the average U8.0 block, 11284 G. The correction factors for these effects are 0.8 % and 1.0 %, respectively. The calculations in Table II are based on a remnant field of 11100 G, which means the fields listed are 1.7 % low. Correcting both measured and calculated values to correspond to the real blocks, we obtain a measured field of 1.369 T and a calculated field of 1.337 T. The difference of only 2 % indicates the method of calculation is quite accurate. And, fortunately, the measured values are higher than the calculated values so that we can expect to achieve the predicted performance of the ID. Similar calculations have been made for the TOK, the BLX device at SSRL, and more recently for the ALS U5.0 undulator. In all cases the calculated fields were slightly lower than the measured values.

Construction Tolerances

A theory developed by Halbach [4] allows us to evaluate the impact of various construction imperfections on the integrated magnetic field on axis in the insertion device, taking into account the three-dimensional structure of the device. The method depends on numerical values of the vector and scalar potentials in the region of the construction error. Several POISSON runs with different boundary conditions are needed to obtain the vector potential at the locations that are identified in Figs. 10a and 10b. The results of these calculations, which are listed in Table.IIIa-c, are the input parameters for a procedure to assign an engineering tolerance to each construction error so that the total rms-error field due to steering errors is less than 0.3% [1], which is set by U8.0 spectral performance requirements. The procedure was applied to ALS U5.0 and ALS U8.0 [10].

By assigning the following tolerances we were able to achieve a steering error of about 0.2% for the ALS U8.0 undulator.

Easy Axis Misorientation	±3	deg
Gap Tolerance	30	μm
Longitudinal Pole Thickness	50	μm
Lateral Pole Width	100	μm
Air Gap between CSEM and Pole	100	μm

Conclusions

Based on a theory of insertion device design developed by Halbach [4], we have determined the parameters of the periodic structure for the 4.5 m long, 8.0 cm period insertion device U8.0 for the ALS at LBL. The parameters of the device are discussed in detail in a conceptual design report [1], and it should easily meet the eventual user requirement of a minimum photon energy of 10 eV.

References:

[1] "U8.0 Undulator Conceptual Design Report," PUB-5276, (May 1990).

[2] ALS Handbook, Rev. 2, PUB-643, (April 1989).

[3] "U5.0 Undulator Conceptual Design Report," PUB-5256, (November 1989).

[4] K. Halbach, "Insertion Device Design," 16 lectures presented from October 1988 to March 1989, PUB V 8811-1.1-16.

[5] POISSON is an improved version of TRIM (A.M.Winslow, *J. Computer Phys.* 1, 149, [1967]) that was developed by K. Halbach et al. PANDIRA is a modified version of POISSON, it allows the solution of permanent magnet and residual field problems.

[6] R. Savoy, "QUICKFIELD, a spread sheet application for hybrid insertion device design," to be published as an ALS Light Source Note.

[7] M. I. Green, D. v. Dyke, "Permeability Measurements of ASTM-A36 Steel, Vanadium Permendur and AISI C 1006 steel," LBID-1675, Berkeley (1991).

[8] W. V. Hassenzahl, D. Phelan "Tests of a Model Pole for the U8.0 Undulator," LBL-31960, Berkeley (1991).

[9] W. V. Hassenzahl, E. Hoyer, and R. Savoy, "Test of a Model Pole Assembly for the ALS U5.0 Undulator," LBL-30938,Berkeley, (June 1991).

[10] R.Savoy, W.V.Hassenzahl, "The ALS U5.0 and U8.0 Magnetic Error Field Calculations," to be published.

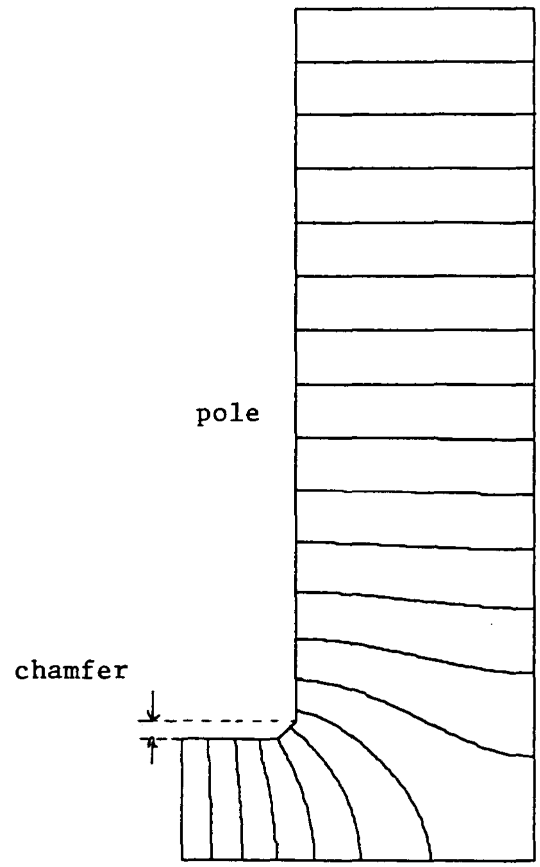

Figure 1: The upper half of a quarter period of an insertion device is shown. This geometry is used for the determination of the spatial harmonics in the aperture. Symmetry of the periodic structure is used to contract the physical extent of the problem, thereby increasing numerical accuracy and speed.

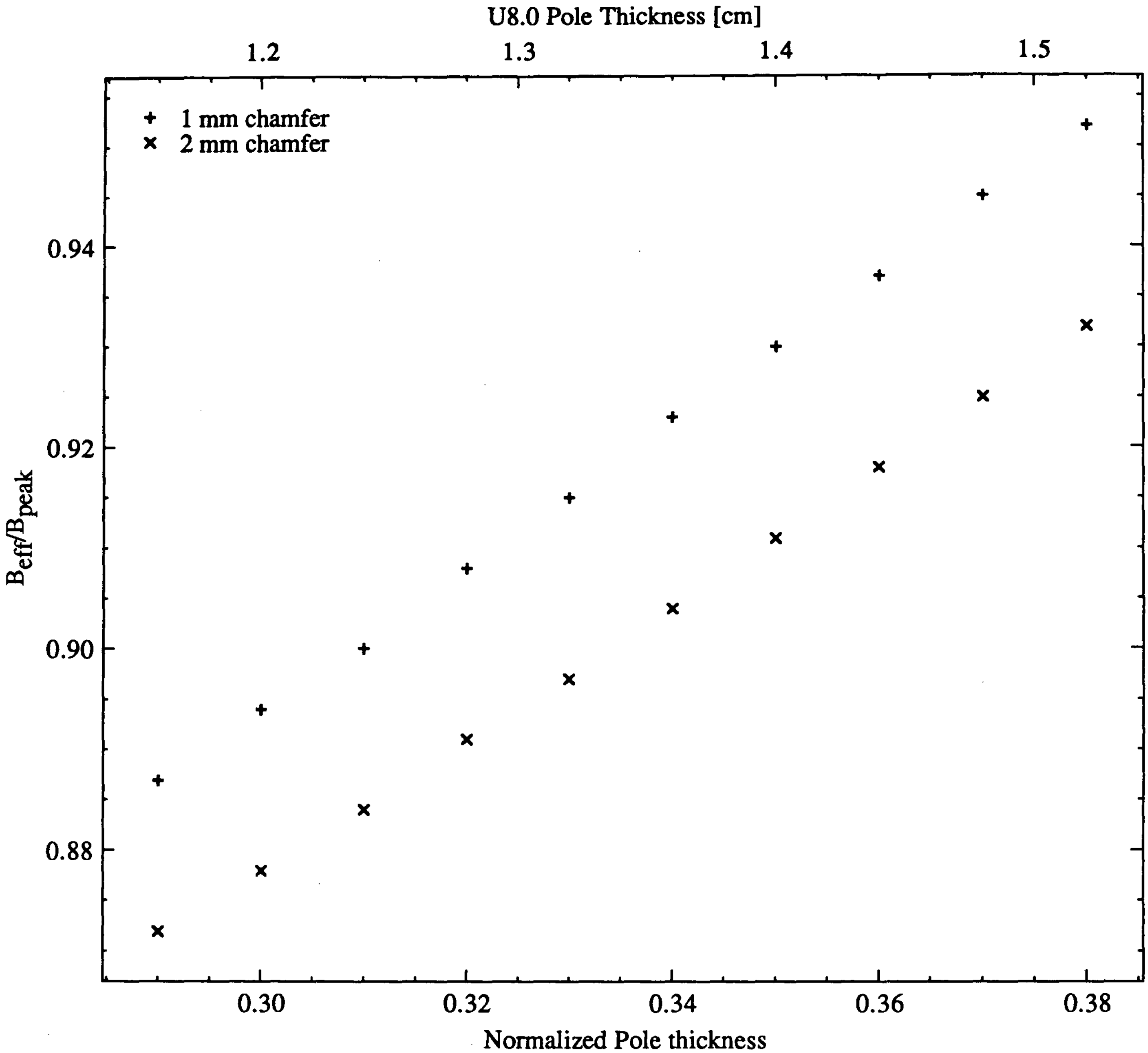

Figure 2: B_{eff}/B_{peak} as a function of normalized pole thickness, p_n, the ratio of full pole thickness p to the length of a half period. The normalized pole thickness selected for U8.0 is 0.32.

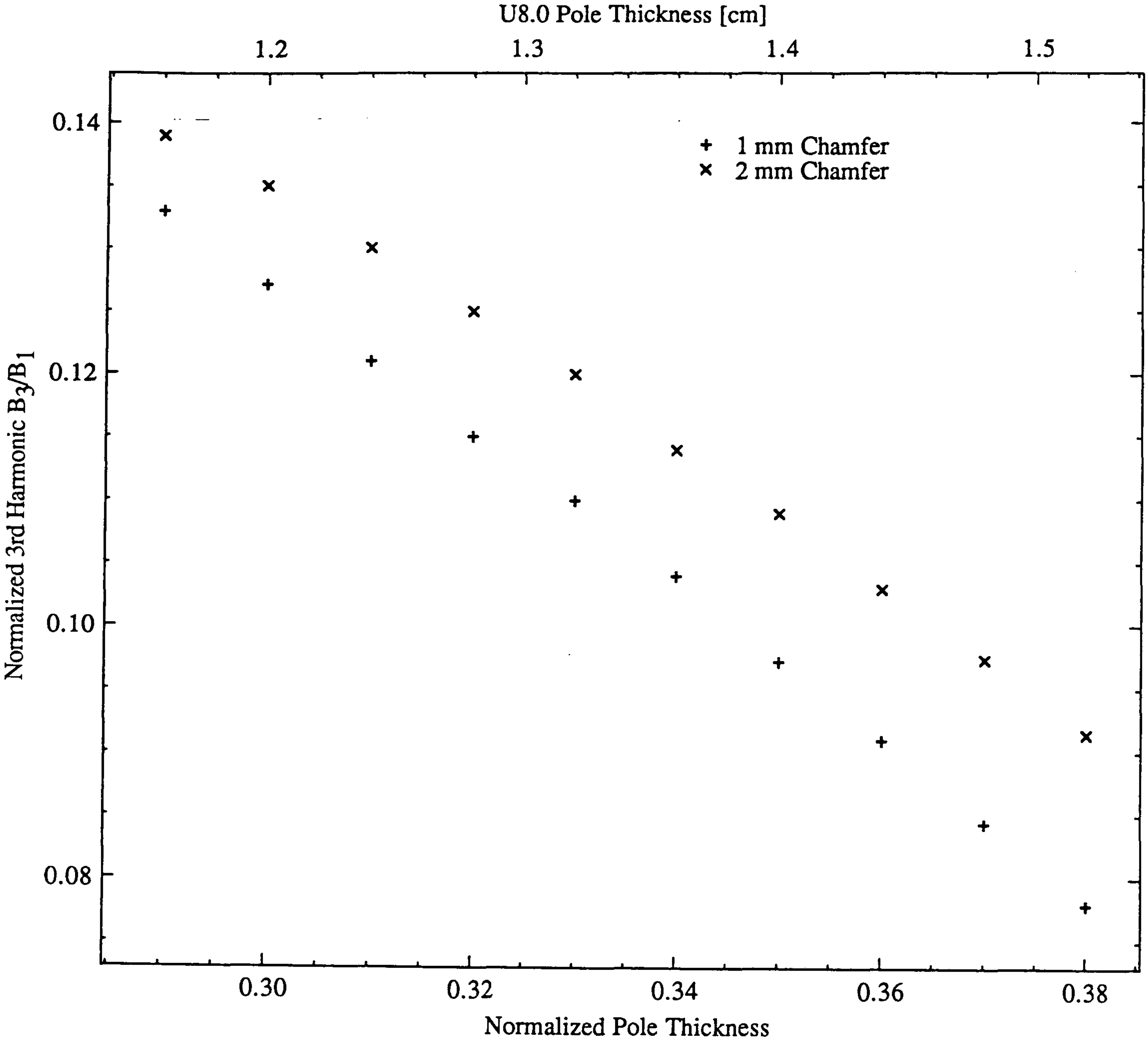

Figure 3: The ratio of the third spatial harmonic to the fundamental at a 1.4 cm gap as a function of normalized pole thickness.

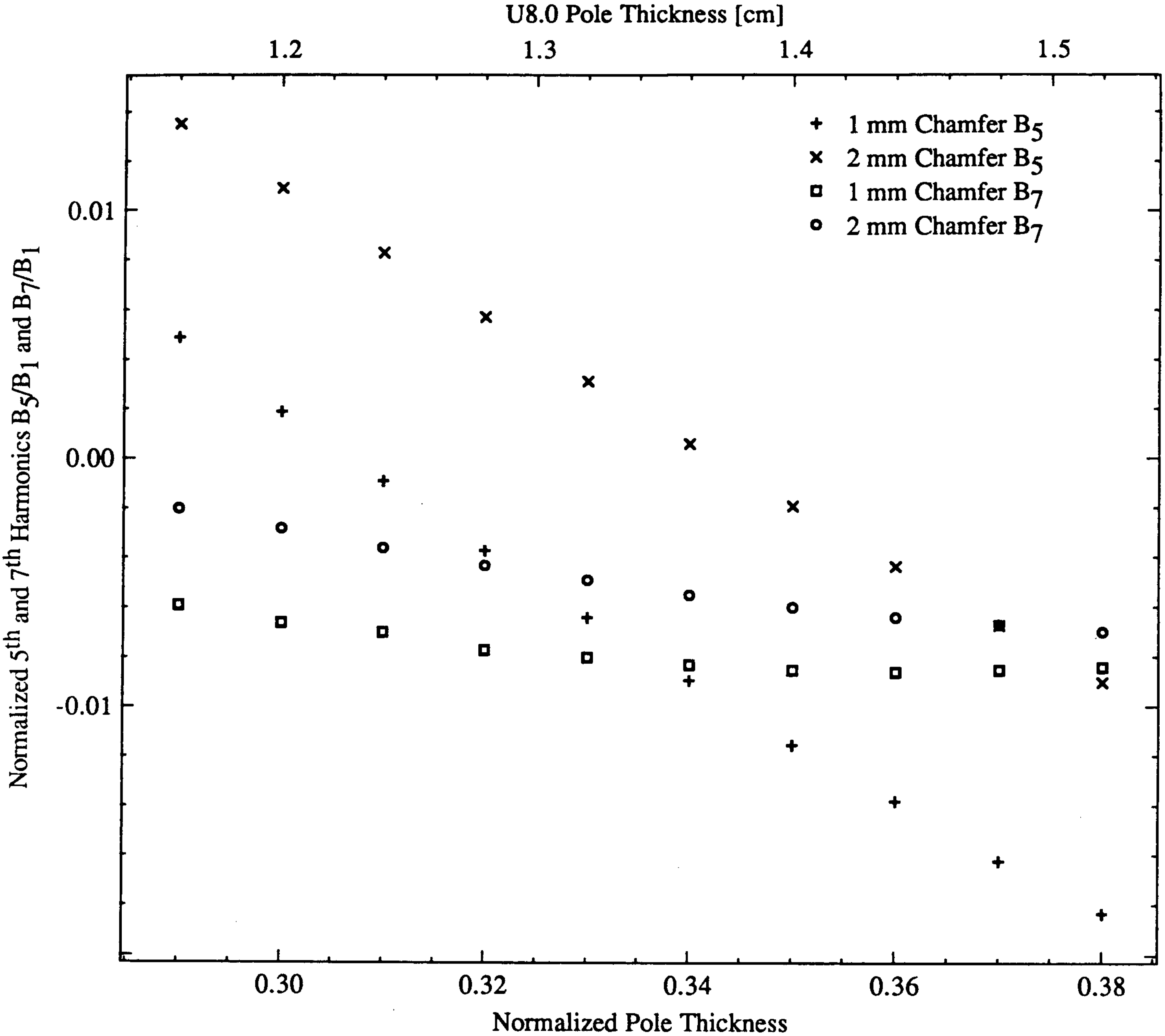

Figure 4: Normalized fifth and seventh spatial harmonic at a 1.4 cm gap as function of normalized pole thickness and chamfer size.

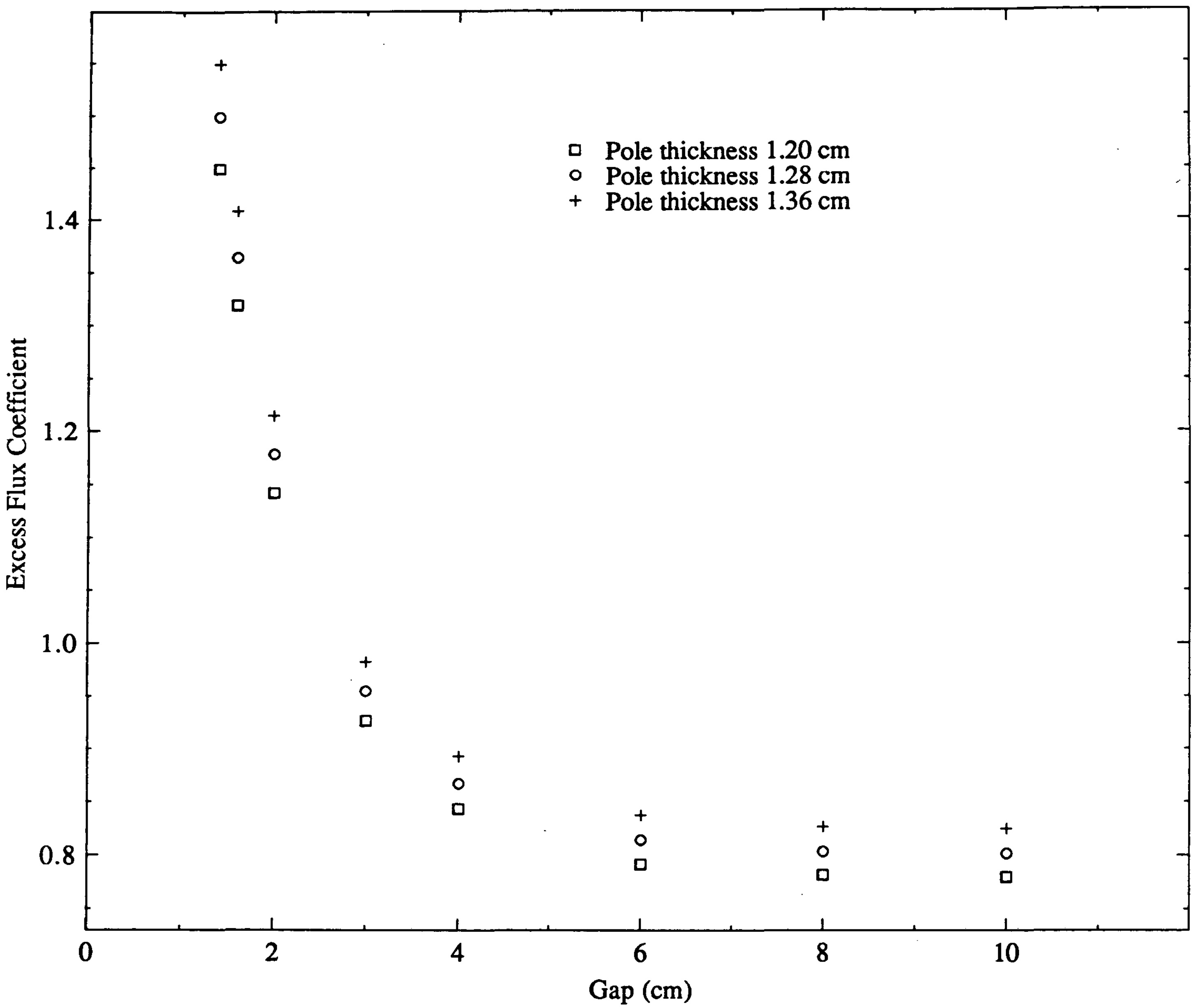

Figure 5: Excess flux coefficient of the pole face as a function of gap.

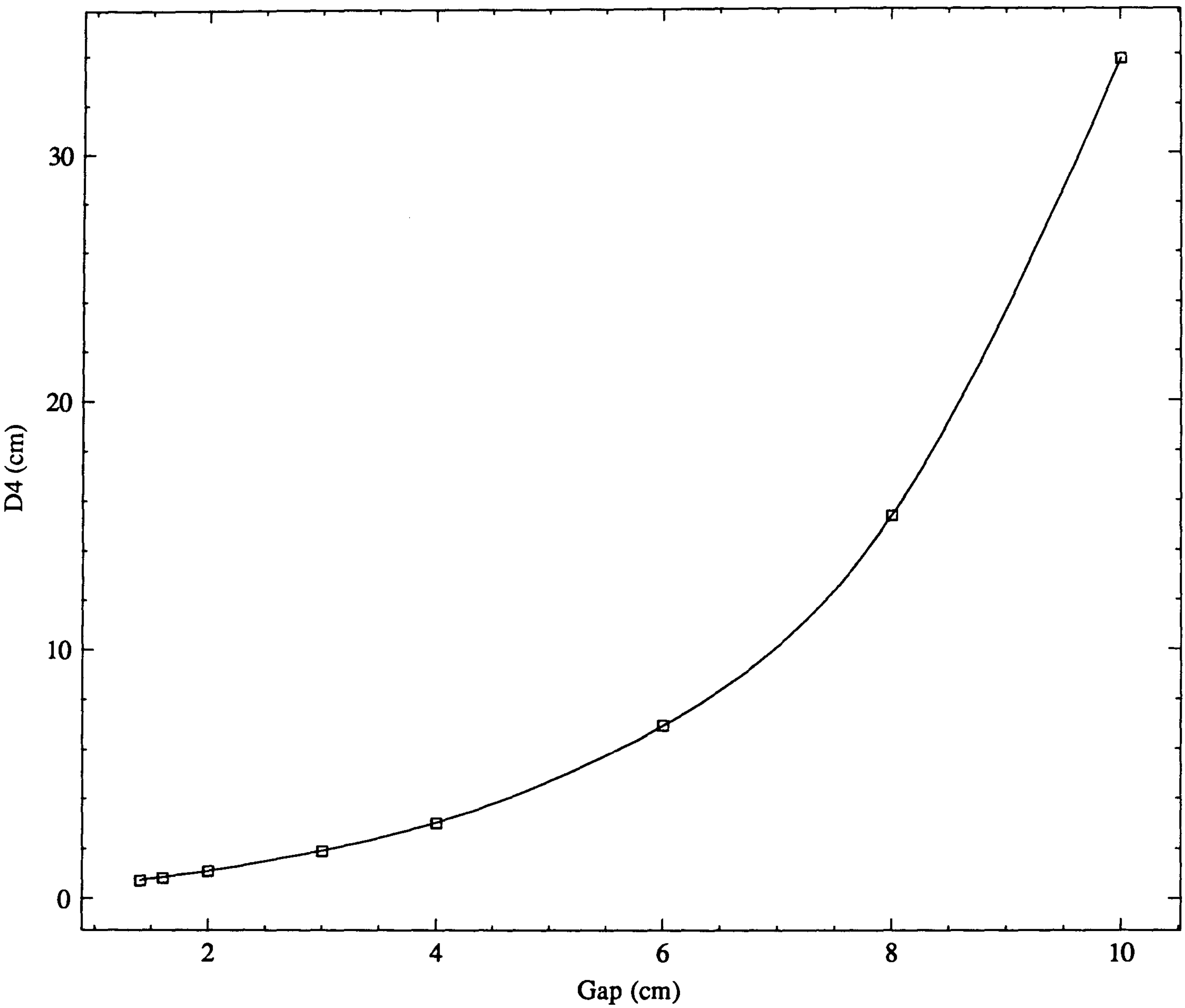

Figure 6: D_4, the scalar potential of the pole divided by the peak field, as a function of gap.

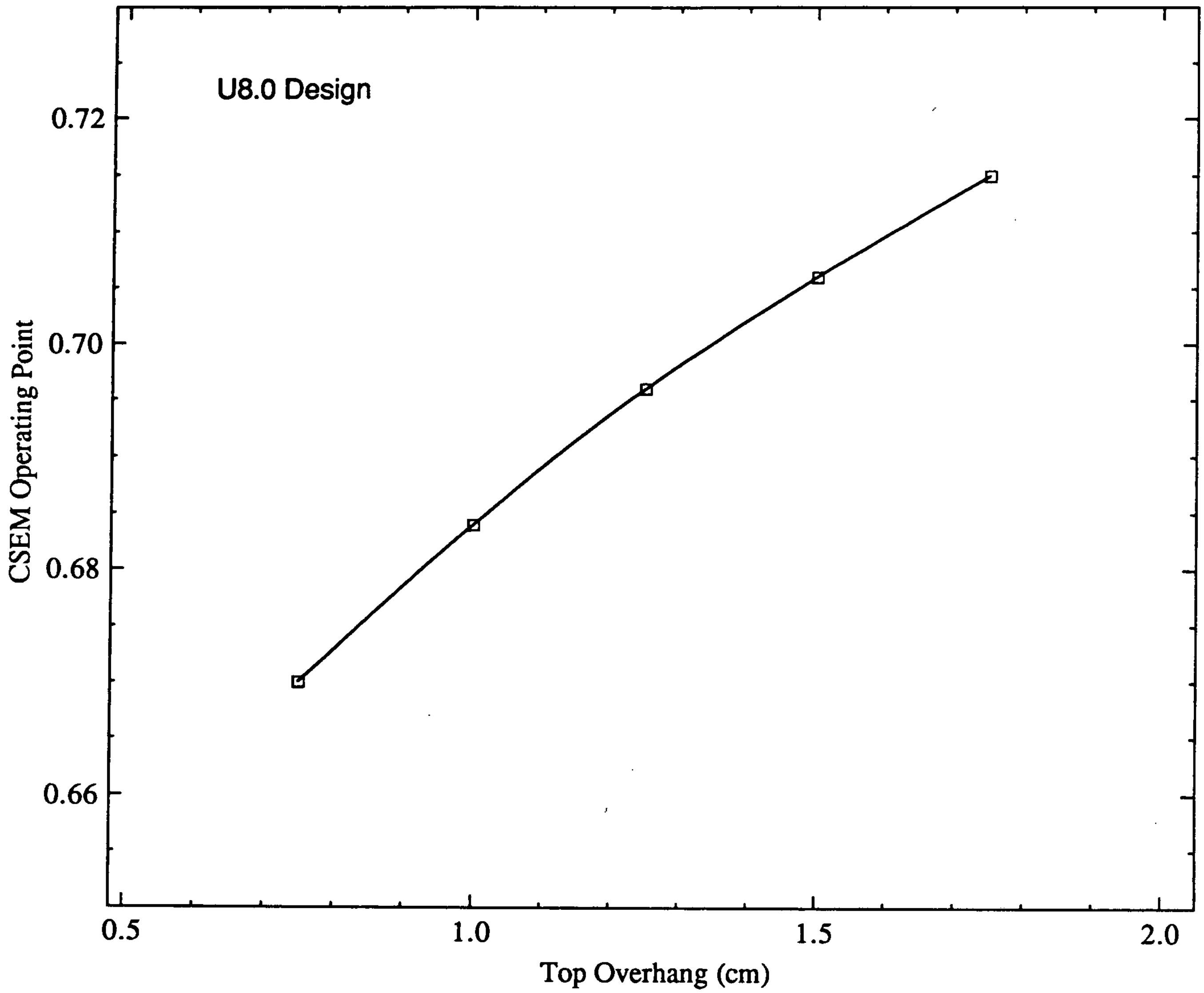

Figure 7: Operating point of the CSEM in U8.0 as function of the top overhang for the selected design: pole thickness = 1.28 cm, pole height = 6.00 cm, and side overhang = 1.25 cm.

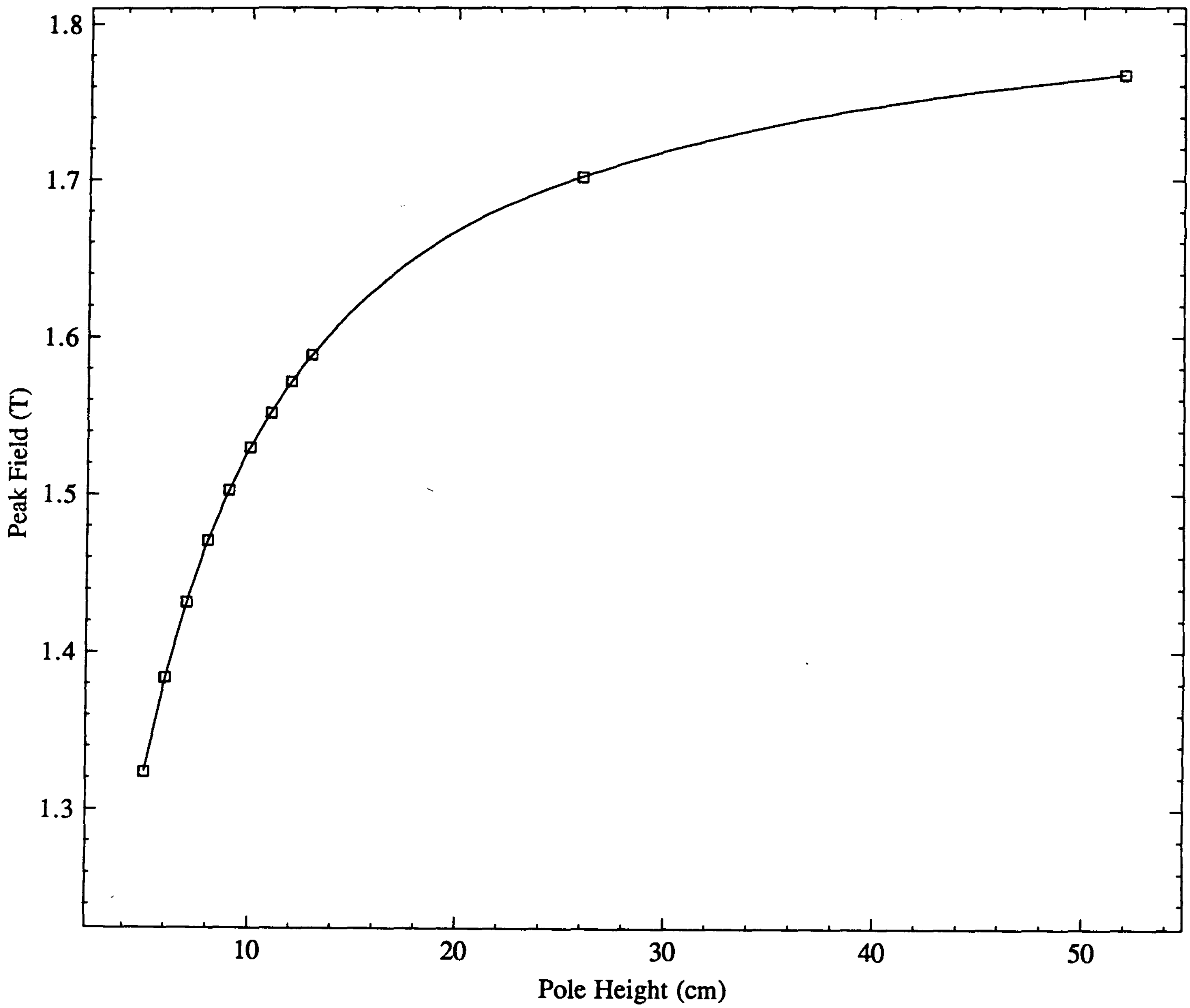

Figure 8: Peak field vs. pole height for an infinite-permeability pole for: gap = 1.4 cm, pole thickness = 1.28 cm, top overhang = 1.20 cm, side overhang = 1.25 cm, and B_r = 11100 G.

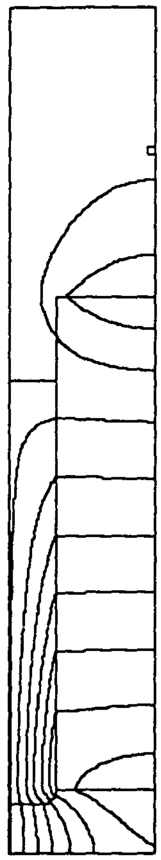

Figure 9: Full height PANDIRA model for U8.0 for: gap = 1.4 cm, pole thickness = 1.28 cm, top overhang = 1.20 cm, and B_r = 11100 G.

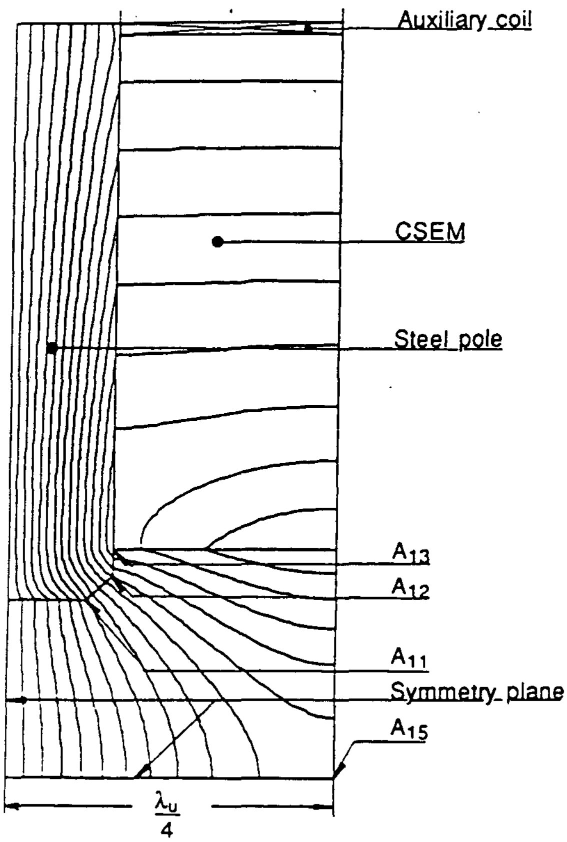

Fig. 10 a

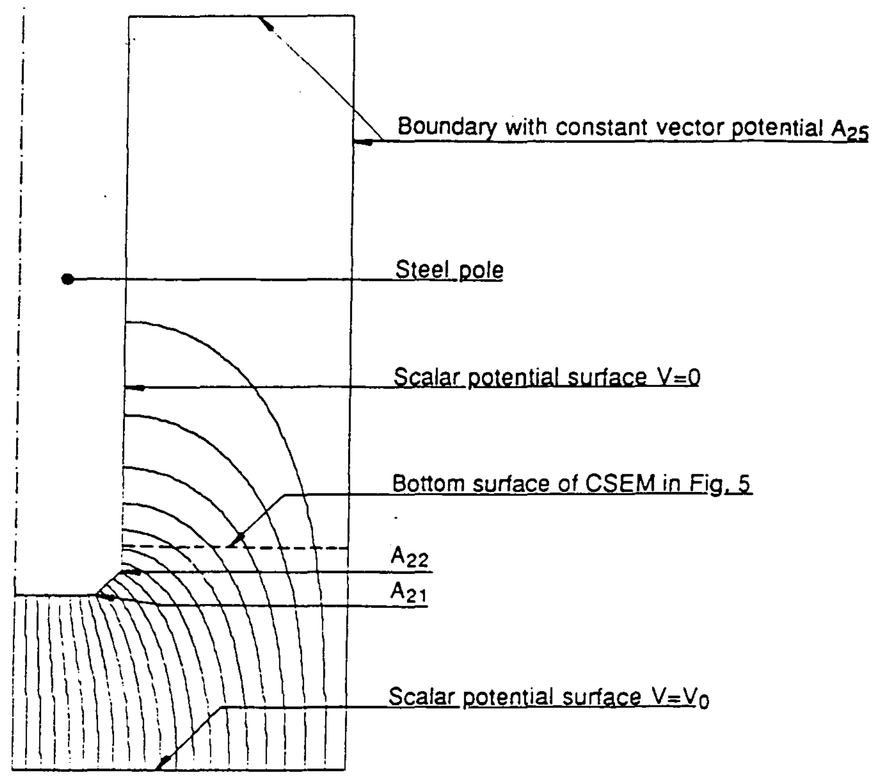

Fig. 10 b

Figure 10: A typical geometry for the calculation of D_4 and the vector potentials A_{11}, A_{12} and A_{13} ('run#1') is shown in Fig. 10a.
The vector potentials A_{21}, A_{22} and A_{23} are determined with the same geometry but modified boundary conditions (Fig. 10b, 'run#2').

1 mm chamfer:

Pole thickness (cm)	normalized Pole thickness	B_3/B_1 1 mm chamfer	B_5/B_1 1 mm chamfer	B_7/B_1 1 mm chamfer	B_{eff}/B_{max} 1 mm chamfer
1.16	.29	0.133	0.0049	-0.0059	0.887
1.20	.30	0.127	0.0019	-0.0066	0.894
1.24	.31	0.121	-0.0009	-0.0072	0.901
1.28	.32	0.115	-0.0037	-0.0077	0.908
1.32	.33	0.110	-0.0064	-0.0080	0.915
1.36	.34	0.104	-0.0089	-0.0083	0.923
1.40	.35	0.097	-0.0115	-0.0085	0.930
1.44	.36	0.091	-0.0138	-0.0086	0.937
1.48	.37	0.084	-0.0162	-0.0085	0.945
1.52	.38	0.078	-0.0183	-0.0084	0.952

2 mm chamfer:

Pole thickness (cm)	normalized Pole thickness	B_3/B_1 2 mm chamfer	B_5/B_1 2 mm chamfer	B_7/B_1 2 mm chamfer	B_{eff} 2 mm chamfer
1.16	.29	0.139	0.0135	-0.0020	0.872
1.20	.30	0.135	0.0109	-0.0028	0.878
1.24	.31	0.130	0.0083	-0.0036	0.884
1.28	.32	0.125	0.0057	-0.0043	0.891
1.32	.33	0.120	0.0031	-0.0049	0.897
1.36	.34	0.114	0.0006	-0.0055	0.904
1.40	.35	0.109	-0.0019	-0.0060	0.911
1.44	.36	0.103	-0.0044	-0.0064	0.918
1.48	.37	0.097	-0.0067	-0.0067	0.925
1.52	.38	0.092	-0.0090	-0.0070	0.932

Table 1: Spatial harmonics and effective field as function of pole thickness. The permeability of the steel pole is infinite for these calculations.

Design of ALS - U8.0 D4 from finite iron pandira run		6/5/90 17:37	U8.0 h=7mm	U8.0 h=7mm	U8.0 h=7mm	U8.0 h=7mm
Variables:			same pole height as U5	U8=U5*1,6	2 layers of square bl.	3 layers
Pole height	D3pole		6.00 cm	9.60 cm	6.20 cm	10.20 cm
Overhang side	(Overside		1.25 cm	2.00 cm	2.00 cm	2.00 cm
Overhang top	(Overtop		1.20 cm	1.92 cm	2.00 cm	2.00 cm
Results						
Field Bo	Bmax		**13153.9 G**	**15195.0 G**	**14067.6 G**	**15351.6 G**
Operating Point of the CSEM	Opoint		0.697	0.805	0.745	0.813
CSEM Volume	csemvolume		44142 ccm	81582 ccm	57655 ccm	86483 ccm
CSEM Price per ccm	csempriceccm		2.50$	2.50$	2.50$	2.50$
CSEM Price Total	csempricetot		**110356$**	**203956$**	**144138$**	**216207$**
Fixed Geometry Data						
Period length Lambda	lambda		8.00 cm	8.00 cm	8.00 cm	8.00 cm
Number of Periods	Nperiods		55.20	55.20	55.20	55.20
Half thickness Pole (longitudinal)	D: polethickness		0.64 cm	0.64 cm	0.64 cm	0.64 cm
Half thickness CSEM (longitudinal)	H: csemthickness		1.36 cm	1.36 cm	1.36 cm	1.36 cm
Dimensional check			OK	OK	OK	OK
Full lateral pole width (in x direction)	2D1 polewidth		8.00	8.00	8.00	8.00
Register distance	I registerheight		0.20	0.20	0.20	0.20
Material Data						
Remanent field of CSEM Br in Gauss	Br		11100 G	11100 G	11100 G	11100 G
Coercive Field of CSEM Hc in Oersted	Hc		10700 Oe	10700 Oe	10700 Oe	10700 Oe
Permeability of CSEM	mue		1.040	1.040	1.040	1.040
Input from 2D calculations						
Halfgap	h		0.70 cm	0.70 cm	0.70 cm	0.70 cm
D4 bad theoretical approximation			0.736	0.736	0.736	0.736
D4 from POISSON or equiv. code	D4 d4poisson		0.771	0.771	0.771	0.771
Excess Flux Coefficients (E.F.C.):			Pandira	Pandira	Pandira	Pandira
Calculated by 2D-Code						
E.F.C. into pole face and side	ep+es		1.499	1.499	1.499	1.499
Calculated analytically						
E.F.C. into top of pole Et	et		0.824	0.824	0.824	0.824
E.F.C. into corner Ec≈0.5	ec		0.500	0.500	0.500	0.500
Analytical Flux coefficients						
Flux into top E01:	AFCe01		0.508	0.645	0.656	0.656
Flux into lateral side E03:	AFCe03		0.520	0.656	0.656	0.656
Flux and Capacitance calculations						
2D-Computer Results used as input						
Run #2: Scalar Potential of Pole	run2_v0		5105.02	5636.6	6675.63	9210
Run #2: Vector potential	run2_A		10000	10000	10000	10000
Run #3: Scalar Potential of Pole	run3_v0		0	0	0	0
Run #3: Scalar pot. Difference A30-A31	run3_A		0	0	0	0
Results						
Total Flux entering one pole (Gauss*sq.cm.)	Fluxtot		667540	1098657	730753	1165134
Integral of complex potential G0	IG0		0.824	0.824	0.824	0.824
Capacitance C2	cap_c2		131.64 cm	187.56 cm	134.75 cm	196.88 cm
Capacitance CF (Pole-Midplane)	cap_cf		31.34 cm	28.39 cm	23.97 cm	17.37 cm
Capacitance Cs (Pole-Side)	cap_cs		#NUM!	#NUM!	#NUM!	#NUM!
Capacitance C1 (Pole to adjacent pole)	cap_c1		#NUM!	#NUM!	#NUM!	#NUM!

Roland Savoy, M.S. 2-400, Lawrence Berkeley Laboratory, Berkeley CA 94720, Phone USA-(415)-486 5963 V9/8

Table IIa: Design spread sheet for minimum gap and finite pole permeability

Design of ALS - U8.0 Corrected Excess flux coefficients E1+E3	4/3/91 9:06	U8.0 h=7mm	U8.0 h=7mm	U8.0 h=7mm	U8.0 h=7mm
Variables:		same pole height as U5	U8=U5*1.6	2 layers of square bl.	3 layers
Pole height	D3pole	6.00 cm	9.60 cm	6.20 cm	10.20 cm
Overhang side	(Overside	1.25 cm	2.00 cm	2.00 cm	2.00 cm
Overhang top	(Overtop	1.20 cm	1.92 cm	2.00 cm	2.00 cm
Results					
Field Bo	Bmax	**13854.7 G**	**16004.6 G**	**14817.1 G**	**16169.6 G**
Operating Point of the CSEM	Opoint	0.697	0.805	0.745	0.813
CSEM Volume	csemvolume	44142 ccm	81582 ccm	57655 ccm	86483 ccm
CSEM Price per ccm	csempriceccm	2.50$	2.50$	2.50$	2.50$
CSEM Price Total	csempricetot	**110356$**	**203956$**	**144138$**	**216207$**
Fixed Geometry Data					
Period length Lambda	lambda	8.00 cm	8.00 cm	8.00 cm	8.00 cm
Number of Periods	Nperiods	55.20	55.20	55.20	55.20
Half thickness Pole (longitudinal)	D: polethickness	0.64 cm	0.64 cm	0.64 cm	0.64 cm
Half thickness CSEM (longitudinal)	H: csemthickness	1.36 cm	1.36 cm	1.36 cm	1.36 cm
Dimensional check		OK	OK	OK	OK
Full lateral pole width (in x direction)	2D1 polewidth	8.00	8.00	8.00	8.00
Register distance	I registerheight	0.20	0.20	0.20	0.20
Material Data					
Remanent field of CSEM Br in Gauss	Br	11100 G	11100 G	11100 G	11100 G
Coercive Field of CSEM Hc in Oersted	Hc	10700 Oe	10700 Oe	10700 Oe	10700 Oe
Permeability of CSEM	mue	1.040	1.040	1.040	1.040
Input from 2D calculations					
Halfgap	h	0.70 cm	0.70 cm	0.70 cm	0.70 cm
D4 bad theoretical approximation		0.736	0.736	0.736	0.736
D4 from POISSON or equiv. code	D4 d4poisson	0.732	0.732	0.732	0.732
Excess Flux Coefficients (E.F.C.):					
Calculated by 2D-Code					
E.F.C. into pole face and side	ep+es	1.499	1.499	1.499	1.499
Calculated analytically					
E.F.C. into top of pole Et	et	0.824	0.824	0.824	0.824
E.F.C. into corner Ec≈0.5	ec	0.500	0.500	0.500	0.500
Analytical Flux coefficients					
Flux into top E01:	AFCe01	0.508	0.645	0.656	0.656
Flux into lateral side E03:	AFCe03	0.520	0.656	0.656	0.656
Flux and Capacitance calculations					
2D-Computer Results used as Input					
Run #2: Scalar Potential of Pole	run2_v0	5105.02	5636.6	6675.63	9210
Run #2: Vector potential	run2_A	10000	10000	10000	10000
Run #3: Scalar Potential of Pole	run3_v0	0	0	0	0
Run #3: Scalar pot. Difference A30-A31	run3_A	0	0	0	0
Results					
Total Flux entering one pole (Gauss*sq.cm.)	Fluxtot	667540	1098657	730753	1165134
Integral of complex potential G0	IG0	0.824	0.824	0.824	0.824
Capacitance C2	cap_c2	131.64 cm	187.56 cm	134.75 cm	196.88 cm
Capacitance CF (Pole-Midplane)	cap_cf	31.34 cm	28.39 cm	23.97 cm	17.37 cm
Capacitance Cs (Pole-Side)	cap_cs	#NUM!	#NUM!	#NUM!	#NUM!
Capacitance C1 (Pole to adjacent pole)	cap_c1	#NUM!	#NUM!	#NUM!	#NUM!

Roland Savoy, M.S. 2-400, Lawrence Berkeley Laboratory, Berkeley CA 94720, Phone USA-(415)-486 5963 V9/8

Table IIb: Design spread sheet for minimum gap and *infinite* pole permeability

Design of ALS - U8.0	4/3/91 9:08	U8.0 h=12mm same pole height as U5	U8.0 h=12mm U8=U5*1.6	U8.0 h=12mm 2 layers of square bl.	U8.0 h=12mm 3 layers of square bl.
Variables:					
Pole height	D3pole	6.00 cm	9.60 cm	6.20 cm	10.20 cm
Overhang side	(Overside	1.25 cm	2.00 cm	2.00 cm	2.00 cm
Overhang top	(Overtop	1.20 cm	1.92 cm	2.00 cm	2.00 cm
Results					
Field Bo	Bmax	**7645.9 G**	**8686.7 G**	**8166.4 G**	**8760.2 G**
Operating Point of the CSEM	Opoint	0.736	0.836	0.786	0.843
CSEM Volume	csemvolume	44142 ccm	81582 ccm	57655 ccm	86483 ccm
CSEM Price per ccm	csempriceccm	2.50$	2.50$	2.50$	2.50$
CSEM Price Total	csempricetot	**110356$**	**203956$**	**144138$**	**216207$**
Fixed Geometry Data					
Period length Lambda	lambda	8.00 cm	8.00 cm	8.00 cm	8.00 cm
Number of Periods	Nperiods	55.20	55.20	55.20	55.20
Half thickness Pole (longitudinal)	D: polethickness	0.64 cm	0.64 cm	0.64 cm	0.64 cm
Half thickness CSEM (longitudinal)	H: csemthickness	1.36 cm	1.36 cm	1.36 cm	1.36 cm
Dimensional check		OK	OK	OK	OK
Full lateral pole width (in x direction) 2D1	polewidth	8.00	8.00	8.00	8.00
Register distance	l registerheight	0.20	0.20	0.20	0.20
Material Data					
Remanent field of CSEM Br in Gauss	Br	11100 G	11100 G	11100 G	11100 G
Coercive Field of CSEM Hc in Oersted	Hc	10700 Oe	10700 Oe	10700 Oe	10700 Oe
Permeability of CSEM	mue	1.040	1.040	1.040	1.040
Input from 2D calculations					
Halfgap	h	1.20 cm	1.20 cm	1.20 cm	1.20 cm
D4 bad theoretical approximation		1.386	1.386	1.386	1.386
D4 from POISSON or equiv. code	D4 d4poisson	1.401	1.401	1.401	1.401
Excess Flux Coefficients (E.F.C.):					
Calculated by 2D-Code					
E.F.C. into pole face and side	ep+es	1.061	1.061	1.061	1.061
Calculated analytically					
E.F.C. into top of pole Et	et	0.824	0.824	0.824	0.824
E.F.C. into corner Ec≈0.5	ec	0.500	0.500	0.500	0.500
Analytical Flux coefficients					
Flux into top E01:	AFCe01	0.508	0.645	0.656	0.656
Flux into lateral side E03:	AFCe03	0.520	0.656	0.656	0.656
Flux and Capacitance calculations					
2D-Computer Results used as input					
Run #2: Scalar Potential of Pole	run2_v0	5105.02	5636.6	6675.63	9210
Run #2: Vector potential	run2_A	10000	10000	10000	10000
Run #3: Scalar Potential of Pole	run3_v0	0	0	0	0
Run #3: Scalar pot. Difference A30-A31	run3_A	0	0	0	0
Results					
Total Flux entering one pole (Gauss*sq.cm.)	Fluxtot	667540	1098657	730753	1165134
Integral of complex potential G0	IG0	0.824	0.824	0.824	0.824
Capacitance C2	cap_c2	124.64 cm	180.55 cm	127.74 cm	189.87 cm
Capacitance CF (Pole-Midplane)	cap_cf	31.34 cm	28.39 cm	23.97 cm	17.37 cm
Capacitance Cs (Pole-Side)	cap_cs	#NUM!	#NUM!	#NUM!	#NUM!
Capacitance C1 (Pole to adjacent pole)	cap_c1	#NUM!	#NUM!	#NUM!	#NUM!

Roland Savoy, M.S. 2-400, Lawrence Berkeley Laboratory, Berkeley CA 94720, Phone USA-(415)-486 5963 V9/8

Table IIc: Design spread sheet for commissioning gap and *infinite* pole permeability

Run #1

Half Gap [cm]	0.70	0.80	1.00	1.50	2.00	3.00	4.00	5.00
Bcenter [G]	2997.58	2690.78	2222.89	822.95	561.23	282.92	149.24	81.30
A15 [Gcm]	3268.05	3008.27	2582.07	1007.29	702.23	358.96	189.89	103.52
A11 [Gcm]	1913.45	1811.81	1679.04	858.69	836.55	901.41	1036.81	1237.38
A12 [Gcm]	2669.32	2551.54	2402.87	1258.69	1241.75	1348.88	1554.38	1855.59
A13 [Gcm]	3080.65	2962.20	2817.78	1498.93	1489.48	1627.44	1877.82	2240.58
Vpole [Gcm]	2212.08	2315.10	2500.69	1591.29	1711.26	1969.25	2297.00	2749.44
Azero [Gcm]	10000	10000	10000	10000	10000	10000	10000	10000
Model height [cm]	5	5	5	9	9	9	9	9
D4 [cm]	0.738	0.860	1.125	1.934	3.049	6.961	15.392	33.821
ln(D4)	-0.30	-0.15	0.12	0.66	1.11	1.94	2.73	3.52
EFC	1.449	1.319	1.142	0.927	0.844	0.792	0.782	0.780

Run #2

Half Gap [cm]	0.70	0.80	1.00	1.50	2.00	3.00	4.00	5.00
Bcenter [G]	7131.60	6791.42	6274.39	5559.02	5250.47	5051.48	5010.68	5002.20
A25 [Gcm]	10000.00	10000.00	10000.00	10000.00	10000.00	10000.00	10000.00	10000.00
A21 [Gcm]	4392.47	4327.43	4247.70	4178.78	4164.98	4161.50	4161.13	4161.00
A22 [Gcm]	5979.40	5915.18	5840.02	5769.48	5756.41	5748.50	5754.25	5749.56
A23 [Gcm]	6752.84	6695.03	6630.81	6567.50	6554.63	6551.06	6550.73	6545.22
Vpole [Gcm]	5211.99	5744.93	6785.74	9321.82	11829.17	16831.13	21831.18	26831.42
Azero [Gcm]	10000	10000	10000	10000	10000	10000	10000	10000
Model height [cm]	9	9	9	9	9	9	9	9
CF (cm) [cm]	30.70	27.85	23.58	17.16	13.53	9.51	7.33	5.96
ln(cf)	3.42	3.33	3.16	2.84	2.60	2.25	1.99	1.79

Table IIIa: Results of POISSON calculations; pole thickness: 1.20 cm

Run #1

Half Gap [cm]	0.70	0.80	1.00	1.50	2.00	3.00	4.00	5.00
Bcenter [G]	1796.85	1587.27	1274.19	811.66	554.31	279.68	147.56	80.39
A15 [Gcm]	1996.20	1802.84	1496.79	998.34	695.10	355.01	187.77	102.36
A11 [Gcm]	1214.14	1128.05	1011.20	883.51	859.16	924.44	1063.38	1269.13
A12 [Gcm]	1666.51	1563.11	1423.27	1275.06	1255.59	1363.56	1572.00	1875.84
A13 [Gcm]	1913.85	1806.01	1660.57	1511.17	1500.09	1637.991	1889.79	2257.57
Vpole [Gcm]	1315.42	1352.65	1416.33	1545.72	1662.45	1913.23	2231.72	2671.39
Azero [Gcm]	10000	10000	10000	10000	10000	10000	10000	10000
Model height [cm]	9	9	9	9	9	9	9	9
D4 [cm]	0.732	0.852	1.112	1.904	2.999	6.841	15.124	33.232
ln(D4)	-0.31	-0.16	0.11	0.64	1.10	1.92	2.72	3.50
EFC	1.499	1.364	1.178	0.955	0.868	0.815	0.804	0.802

Run #2

Half Gap [cm]	0.70	0.80	1.00	1.50	2.00	3.00	4.00	5.00
Bcenter [G]	7033.72	6716.36	6229.12	5544.13	5244.73	5050.42	5010.45	5002.15
A25 [Gcm]	10000.00	10000.00	10000.00	10000.00	10000.00	10000.00	10000.00	10000.00
A21 [Gcm]	4592.37	4526.28	4445.49	4374.89	4360.62	4356.83	4356.88	4355.63
A22 [Gcm]	6147.10	6083.34	6004.36	5934.45	5920.00	5916.25	5925.00	5913.13
A23 [Gcm]	6905.08	6847.90	6777.34	6714.86	6701.96	6698.55	6698.03	6699.31
Vpole [Gcm]	5105.01	5636.60	6675.63	9210.20	11717.36	16719.10	21719.25	26719.53
Azero [Gcm]	10000	10000	10000	10000	10000	10000	10000	10000
Model height [cm]	9	9	9	9	9	9	9	9
CF (cm) [cm]	31.34	28.39	23.97	17.37	13.65	9.57	7.37	5.99
ln(Cf)	3.44	3.35	3.18	2.85	2.61	2.26	2.00	1.79

Table IIIb: Results of POISSON calculations; pole thickness: 1.28 cm

Run #1

Half Gap [cm]	0.70	0.80	1.00	1.50	2.00	3.00	4.00	5.00
Bcenter [G]	1755.01	1552.94	1249.98	799.18	546.63	276.08	145.68	79.38
A15 [Gcm]	1987.14	1792.56	1485.48	988.05	687.05	350.61	185.42	101.09
A11 [Gcm]	1252.17	1162.14	1039.74	905.48	879.04	944.80	1086.69	1296.78
A12 [Gcm]	1692.56	1586.13	1441.98	1288.73	1267.91	1375.09	1586.75	1891.92
A13 [Gcm]	1934.33	1823.84	1674.74	1521.10	1508.55	1646.31	1899.68	2269.16
Vpole [Gcm]	1276.00	1312.37	1374.53	1500.48	1613.95	1857.56	2166.93	2594.05
Azero [Gcm]	10000	10000	10000	10000	10000	10000	10000	10000
Model height [cm]	9	9	9	9	9	9	9	9
D4 [cm]	0.727	0.845	1.100	1.878	2.953	6.728	14.875	32.678
ln(D4)	-0.32	-0.17	0.09	0.63	1.08	1.91	2.70	3.49
EFC	1.549	1.408	1.215	0.983	0.893	0.838	0.827	0.825

Run #2

Half Gap [cm]	0.70	0.80	1.00	1.50	2.00	3.00	4.00	5.00
Bcenter [G]	6934.15	6638.86	6181.27	5527.79	5238.34	5049.23	5010.20	5002.08
A25 [Gcm]	10000.00	10000.00	10000.00	10000.00	10000.00	10000.00	10000.00	10000.00
A21 [Gcm]	4785.97	4719.03	4636.93	4564.95	4550.27	4546.69	4546.56	4546.50
A22 [Gcm]	6305.39	6242.22	6164.29	6094.27	6080.00	6077.50	6070.00	6074.13
A23 [Gcm]	7044.74	6988.71	6919.69	6858.35	6845.69	6842.54	6842.33	6842.53
Vpole [Gcm]	5003.41	5533.48	6570.64	9103.71	11610.45	16612.19	21612.25	26612.46
Azero [Gcm]	10000	10000	10000	10000	10000	10000	10000	10000
Model height [cm]	9	9	9	9	9	9	9	9
CF (cm) [cm]	31.98	28.91	24.35	17.58	13.78	9.63	7.40	6.01
	3.47	3.36	3.19	2.87	2.62	2.27	2.00	1.79

Table IIIc: Results of POISSON calculations; pole thickness: 1.36 cm pole thickness: 1.28 cm

overhang side: 1.20 cm

half gap: 0.7 cm

overhang top (cm)	Center Field (Gauss)	Material Volume (cm^3) CSEM	Operating Point
0.75	13310.4	39938	0.670
1	13603.5	42040	0.684
1.25	13844.4	44142	0.696
1.5	14042.3	46244	0.706
1.75	14204.9	48346	0.715

half gap (cm)	d4	excess flux coefficient
0.7	0.732	1.499
0.8	0.852	1.364
1	1.112	1.178
1.5	1.904	0.955

Table IV: Peak field, total CSEM volume and operating point for various top overhangs. An infinite pole permeability was used.

LAWRENCE BERKELEY LABORATORY
UNIVERSITY OF CALIFORNIA
TECHNICAL INFORMATION DEPARTMENT
BERKELEY, CALIFORNIA 94720